*THINK INDIA JOURNAL*

ISSN: 0971-1260

Vol-22-Issue-17-September-2019

# Computer Simulation Through Diffuse Interface of Two Grains of Circular Geometries in 2D

**Prashant Bagde[1*], Jaspreet Singh[1], Mandeep Singh,**

[1]*School of Mechanical Engineering, Lovely Professional University, Phagwara, Punjab, India*

*Corresponding Author: prashant.bagde@lpu.co.in

**Abstract**

A grain is a crystal within the polycrystal, which usually does not have a regular shape; and, a grain boundary is a zone of transition between different crystalline orientations of the adjacent grains. Here we discuss the diffuse-interface description for movement of grain boundaries and assurity of the diffuse interface field model in explaining curvature driven micro-structural evolutions. In this study, we only consider two dimensional systems with isotropic grain boundary energy. Specifically, we report results from our studies on two grains of circular geometries in 2-D and the effect of various simulation parameters on the results. There are a variety of computer simulation methods to study grain growth; for example, models such as boundary dynamics model, vertex models, Potts model, Voronoi tessellation and models based on mean field theories (see Ref. 9). In this report, we use diffuse-interface models of the type proposed by Chen and co workers (see Ref. 9-11). In this section we summarise the salient features of as well as some of the pertinent results from the diffuse interface models.

## 1. Introduction

A grain is a crystal within the polycrystal, which usually does not have a regular shape; and, a grain boundary is a zone of transition between different crystalline orientations of the adjacent grains.

Grain boundaries are regions of disorder. This disorder results in an increase in the internal energy due to the broken, unsatisfied or unequilibrated bonds at the grain boundaries. However the increase in the entropy associated with the disorder at the grain boundary is not large. Hence, as compared to a single crystal, a polycrystal with grain boundaries has a higher (positive excess) free energy. So, grain limit movement happens in polycrystalline materials to

ISSN: 0971-1260

Vol-22-Issue-17-September-2019

decrease the all out grain limit region and the abundance free vitality related with them; this procedure is alluded to as grain development

In polycrystalline materials the microstructure, i.e, the sizes, shapes and strategy of grains, essentially chooses the mechanical properties; for instance, using an equation like Hall–Petch, it can be shown that the yield stress is inversely proportional to the grain size. So, as the grains become smaller and smaller, the material becomes more and more strong. Hence grain growth can lead to changes in the properties of the materials and is an important area of study both from an industrial and fundamental points of view.

**Some salient analytical results**

According to Neumann and Mullins (Ref. 2-3), in 2-dimensions, the individual grain area change with respect to time doesn't rely upon the size or geometrical state of the grain, however depends just on its number of sides. This condition is applicable at the points where three grains meet the boundaries make an angle of $120^{o}$:

$$\frac{da}{dt} = \frac{m\gamma\pi}{3}(n-6), \qquad (1.1)$$

where $a$ and n are the area and the number of sides of grains, γ and m are the energy of the grain boundaries and mobility.

- Grains grow when n > 6; that is, when the number of sides of grain are greater than six.
- Grains contract when n < 6; that is, when the number of sides are less than six.
- Grains neither grow nor contract if n = 6; that is, when the number of sides are six.

The above result of Neumann and Mullins can also be understood if we consider the grain growth as a curvature driven process. If a grain boundary is curved, the atoms on the concave side have lower potential than those on the convex side. That is, the atoms are less tightly bound by neighbouring atoms on the convex surface. Thus, if the system is kept at a high enough temperature which gives enough mobility, thermal movements will gradually transfer the atoms from the grain with a more convex surface to a grain with a more concave surface. Since little grains will in general have surfaces with more

ISSN: 0971-1260

Vol-22-Issue-17-September-2019

keen convexity, they will progressively vanish by nourishing the bigger grains. The net impact is grain development.

In interface motion theories, the grain boundary motion in term of speed V given by

$$V = B\Delta u,$$

$$V = B\sigma_{gb}\Omega(\lambda_1 + \lambda_2), \qquad (1.2)$$

where, $\Delta u$ = Chemical potential difference per atom across the boundary.

$\Omega$ = Atomic volume

$B$ = Mobility

$\lambda_1 + \lambda_2$ = Mean curvature

$\sigma_{gb}$ = Grain boundary energy

**Diffuse interface modeling of normal grain growth**

Both experimentally and from simulations, it is known that grain growth can in general be classified as of two types: normal and abnormal grain growth; see for example (Ref. 4). As shown schematically in Fig. 1.1 and 1.2 below, under normal growth of grain, the size of grains increases slowly, and the grain size distribution is unimodal. During abnormal grain growth the mean grain size changes first a little, if at all, and thereby increase rapidly; the initial stage of very little or no growth is known as incubation period. In this report, we only study normal grain growth.

There are many different types of models of grain growth. These can broadly be classified as atomistic and continuum models. Continuum models may again be broadly classified as sharp and diffuse interface models. In the sharp-interface models the grain limits are

ISSN: 0971-1260

Vol-22-Issue-17-September-2019

unique geometrical surfaces having properties, for example, region, bend, free energy, and portability. Such models are reviewed in (Ref. 5-7).

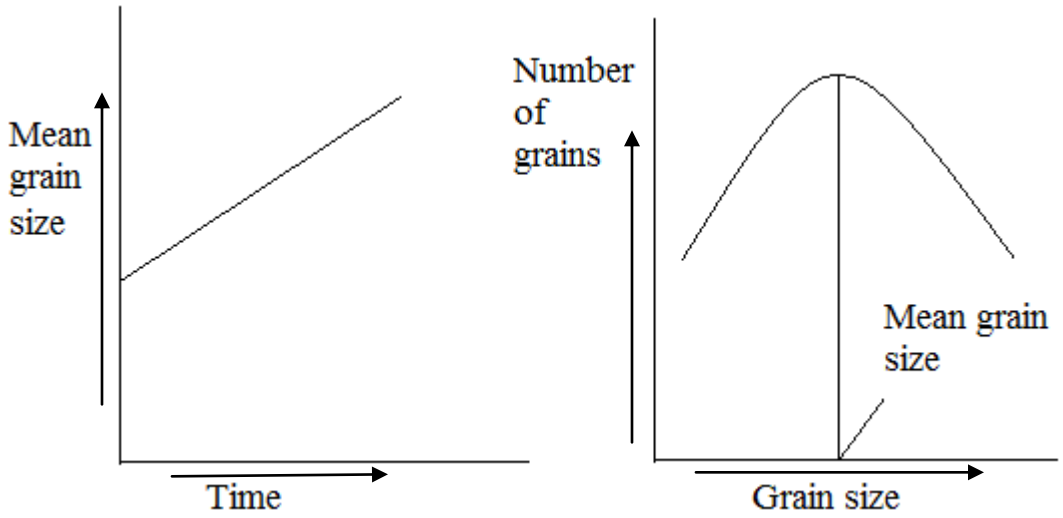


Fig.1.1 Normal grain growth

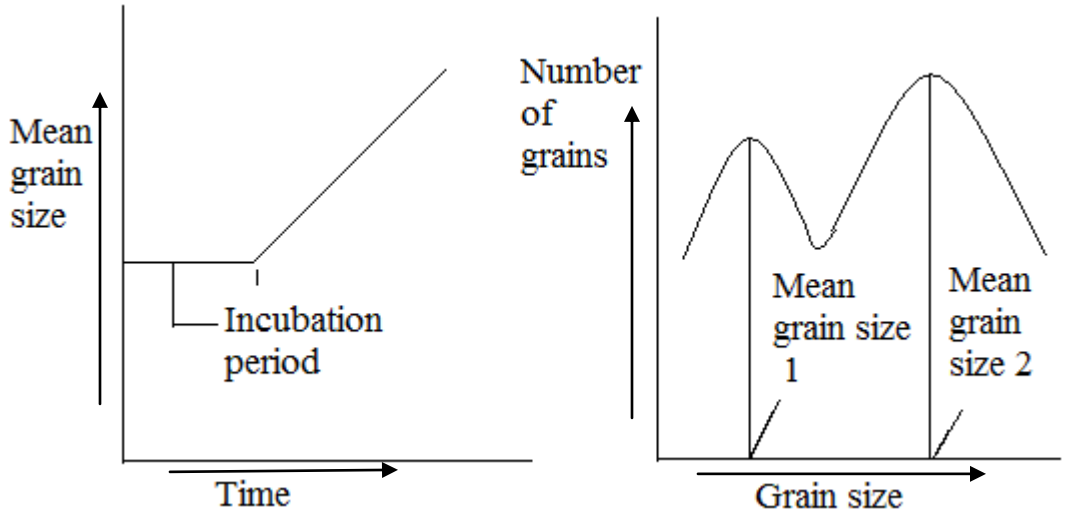


Fig.1.2 Abnormal grain growth

In diffuse interface model the main feature is diffuse of grain boundaries with limited thickness. This is like the hypothetical treatments of anti-phase space limits by Allen and Cahn (see Ref. 8).

The grain limit vitality is naturally presented through the inclination vitality. As fundamental preferences approach is that a self-assertive microstructure can be often treated as the inter-faces are not solitary surfaces requiring inconvenience of moving limit conditions as in the sharp-interface depiction, however only a district where the fields have high slopes (see Ref. 9).

## 2. Theoretical Formulation and Numerical Implementation

In the diffuse interface model, a polycrystalline microstructure is described by as many orientation field variables as there are distinct grains (see Fig. 2.1 below where we schematically show the description of a system with seven grains); these field variables distinguish the different orientations of the grains and are continuous functions of spatial position and time. For every grain, the corresponding orientation field variable has a constant value of unity inside the grain but changes to zero outside the grain over the thickness of the grain boundary. The worldly development of these field factors, and hence the microstructural advancement and grain development energy are described by the time-dependent Ginzburg- Landau (TDGL) equations.

### 2.1 The diffuse-interface model

Let us consider an polycrystalline microstructure as a set of orientation field variables,

$$\eta_1(r), \eta_2(r), ..., \eta_p(r),$$

where p is the number of possible orientations. The total free energy of such a system in terms of all the orientation field variables and their gradients can be written as:

$$F = \int [ f_o(\eta_1(r), \eta_2(r), ..., \eta_p(r)) + \sum_{i=1}^{p} \frac{k_i}{2} (\nabla \eta_i(r))^2 ] d^3 r \qquad (2.1)$$

where i=1, 2,…,p, and $f_0$( free local energy density as a component of field variables $\eta_i$), and $k_i$ ( gradient energy coefficients).

 

ISSN: 0971-1260

Vol-22-Issue-17-September-2019

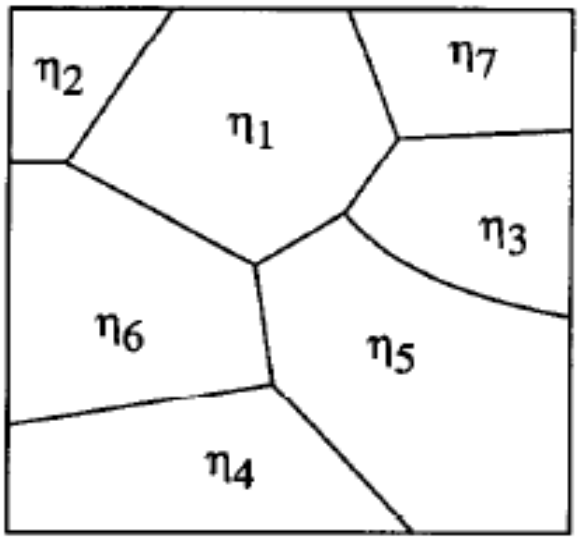


Fig.2.1.Diagram of microstructure showing 7 grains using 7 orientation field variables

In present study, to begin with, we consider the two grain case of one grain embedded in another; hence, there are two continuous field variables $\eta_1$ and $\eta_2$, corresponding to the two orientations. In such a case, the free total energy of the inhomogeneous system as a function of the two orientation field variables and their gradients is:

$$F = \int [ f_o(\eta_1(r), \eta_2(r)) + \sum_{i=1}^{2} \frac{k_i}{2} (\nabla \eta_i(r))^2 ] d^3 r \, . \qquad (2.2)$$

The main requirement for $f_0$ ***is that it has two (since p=2) degenerate minima with equal depth,*** $f_{\min}$ located at ($\eta_1, \eta_2$) = (1, 0), and (0, 1) in the 2- dimensional space.

ISSN: 0971-1260

Vol-22-Issue-17-September-2019

Since the direction field factors are non-rationed amounts, their neighborhood development rates are straightly relative to the variational subsidiary of the all out free vitality as for the nearby direction field variable, i.e. governed by the Ginzburg - Landau equations,

$$\frac{\partial \eta_i(r,t)}{\partial t} = -L_i \frac{\delta F}{\delta \eta_i(r,t)}, \qquad \text{i=1, 2,…,p} \qquad (2.3)$$

where $L_i$ is Relaxation coefficients, t is time and F is Free total energy ). For the two grain case we have two equations:

$$\frac{\partial \eta_1(r,t)}{\partial t} = -L_1 \frac{\partial F}{\partial \eta_1(r,t)}$$

$$\frac{\partial \eta_2(r,t)}{\partial t} = -L_2 \frac{\partial F}{\partial \eta_2(r,t)}$$

If we substitute for the free energy expression in the above equations, we obtain the equations for the evolution.

Thus, for our case, the evolution of the orientational order parameter fields $\eta$ are described by,

$$\frac{\partial \eta_1(r,t)}{\partial t} = -L_1 \frac{\partial}{\partial \eta_1(r,t)} [\int [ f_0(\eta_1, \eta_2) + \frac{k_1}{2} (\nabla \eta_1)^2 + \frac{k_2}{2} (\nabla \eta_2)^2 ]] d^3 r \,,$$

$$\frac{\partial \eta_2(r,t)}{\partial t} = -L_2 \frac{\partial}{\partial \eta_2(r,t)} [\int [ f_0(\eta_1, \eta_2) + \frac{k_1}{2} (\nabla \eta_1)^2 + \frac{k_2}{2} (\nabla \eta_2)^2 ]] d^3 r \,,$$

ISSN: 0971-1260

Vol-22-Issue-17-September-2019

Putting $$f_0(\eta_1,\eta_2) = -\frac{\alpha}{2}(\eta_1^{\,2}+\eta_2^{\,2}) + \frac{\beta}{4}(\eta_1^{\,4}+\eta_2^{\,4}) + 2\gamma(\eta_1^{\,2}\eta_2^{\,2}), \qquad (2.4)$$

where $\alpha$, $\beta$ and $\gamma$ are positive constants

we obtain, 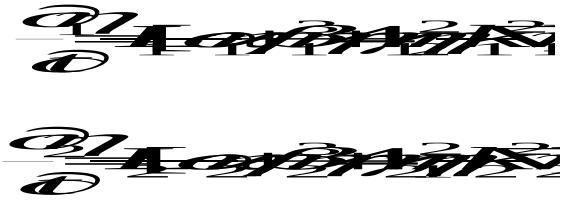 .

**Initial and boundary conditions**:

In our model calculations, when we embed a grain inside another, for the initial profile (that is, profile at t=0) of the continuous field variables $\eta_1$ and $\eta_2$, we assume the following: $\eta_1$ is unity in the embedded grain (while $\eta_2$ is 0) while it is the other way around for the other grain.

$\eta_1(x,t=0)=1$ and $\eta_2(x,t=0)=0$ only inside the embedded grain.

On the outside of the embedded grain $\eta_1(x,t=0)=0$ and $\eta_2(x,t=0)=1$. We use periodic boundary conditions on the simulation domain which is the natural boundary condition to use since our numerical implementation is based on Fourier transforms as described below.

**2.2 Numerical implementation**

We use a semi-implicit Fourier spectral technique to solve the equations of microstructural evolution. To do so, we first (spatially) Fourier transform the evolution equations, and use a forward difference scheme for the time evolution.

$$\frac{\partial \eta_1}{\partial t} = \frac{\eta_1^{t+\Delta t} - \eta_1^{t}}{\Delta t}, \tag{2.5}$$

$$\frac{\partial \eta_1}{\partial t} = L_1 \alpha \eta_1 + k_1 L_1 \nabla^2 \eta_1 - L_1 \beta \eta_1^{3} - 4 L_1 \gamma \eta_1 \eta_2^{2}.$$

Similarly,

$$\frac{\partial \eta_2}{\partial t} = L_2 \alpha \eta_2 + k_2 L_2 \nabla^2 \eta_2 - L_2 \beta \eta_2^{3} - 4 L_2 \gamma \eta_2 \eta_1^{2}.$$

Taking $h_1(\eta_1, \eta_2) = -L_1 \beta \eta_1^{3} - 4 L_1 \gamma \eta_1 \eta_2^{2}$, and,

$$h_2(\eta_1, \eta_2) = -L_2 \beta \eta_2^{3} - 4 L_2 \gamma \eta_2 \eta_1^{2}$$

we obtain,

$$\frac{\partial \overset{\circ}{\eta}_1}{\partial t} = L_1 \alpha \overset{+}{\eta}_1 + k_1 L_1 \nabla^2 \overset{+}{\eta}_1 + \overset{\sim}{h_1}(\eta_1, \eta_2), \tag{2.6}$$

where,

$$\nabla \overset{+}{\eta}_1 = -i\kappa \overset{+}{\eta}_1$$

$$\nabla \nabla \overset{+}{\eta}_1 = (-i)^2 \kappa^2 \overset{+}{\eta}_1 = -\kappa^2 \overset{+}{\eta}_1$$

$$\frac{\overset{+}{\eta}_1^{t+\Delta t} - \overset{+}{\eta}_1^{t}}{\Delta t} = L_1 \alpha \overset{+}{\eta}_1^{t+\Delta t} - k_1 L_1 \kappa^2 \overset{+}{\eta}_1^{t+\Delta t} + \overset{\sim}{h_1}(\eta_1, \eta_2)^{t}$$

$$\frac{\overset{+}{\eta}_2^{t+\Delta t} - \overset{+}{\eta}_2^{t}}{\Delta t} = L_2 \alpha \overset{+}{\eta}_2^{t+\Delta t} - k_2 L_2 \kappa^2 \overset{+}{\eta}_2^{t+\Delta t} + \overset{\sim}{h_2}(\eta_1, \eta_2)^{t}$$

Finally, we get

ISSN: 0971-1260

Vol-22-Issue-17-September-2019

$$\eta_1^{t+\Delta t} = \frac{\eta_1^{t} + \widetilde{h_1}(\eta_1,\eta_2)^{t}}{1+\Delta t(-L_1\alpha + k_1 L_1 \kappa^2)}, \qquad (2.7)$$

and $$\eta_2^{t+\Delta t} = \frac{\eta_2^{t} + \widetilde{h_2}(\eta_1,\eta_2)^{t}}{1+\Delta t(-L_2\alpha + k_2 L_2 \kappa^2)}.$$

**Coding**

The following results are obtained using a C code which is a modified version of a code of M. P. Gururajan, which is available online (see Ref. 13). I have downloaded this code, which is meant for solving the Allen-Cahn equations for order-disorder transformations (using the freeware fastest fourier transform to the west of pacific-- FFTW).We modified it to do grain growth simulations for one grain inside the another. This modification involves, changing the initial conditions in this program, modifying the formulation with increased numbers of parameters (two instead of one), and, doing the calculations for two orientation field variables instead of one.

**Simulation parameters**

In all our simulations we use the following values for the various parameters (unless specified otherwise).

**Table 2.1 Simulation parameters**

| **Case :** | $n\_x = n\_y$ | **256** | **512** | **1024** |
|---|---|---|---|---|
| | $\Delta x = \Delta y$ | **1** | **0.5** | **0.25** |
| | $\alpha = \beta = \gamma$ | **1** | **1** | **1** |

ISSN: 0971-1260

Vol-22-Issue-17-September-2019

| | | | | |
|---|---|---|---|---|
| **A.Circular** | $k_1 = k_2$<br><br>$L_1 = L_2$ | **1**<br><br>**1** | | |

## 3. Results and discussions

In this report, we discuss the time evolution of circular grain boundary in different embedded grains:

### 3.1 Microstructures

In Fig. 3.1 (a-d), we show the evolution of microstructural for a grain with circular boundaries embedded in another; while the circular ones move in such a way that as time proceeds the embedded grains decrease in area; finally, they will disappear leaving behind a single grain. This trend is in agreement with what we expect from the curvature driven growth. Further, the differences in time for the complete disappearance of the embedded grains in the circular cases is a reflection of the differences in the mean curvature at various points on the boundary in these cases; while the curvature is the same at all points on the circular boundary. Finally, while the circular grain remains circular at all times. This is also expected because we have assumed isotropic grain boundary energy and hence for a given area a circular shape minimizes the grain boundary length.

Fig.3.1.Microstructural evolution for a grain with circular boundaries embedded in another.

ISSN: 0971-1260

Vol-22-Issue-17-September-2019

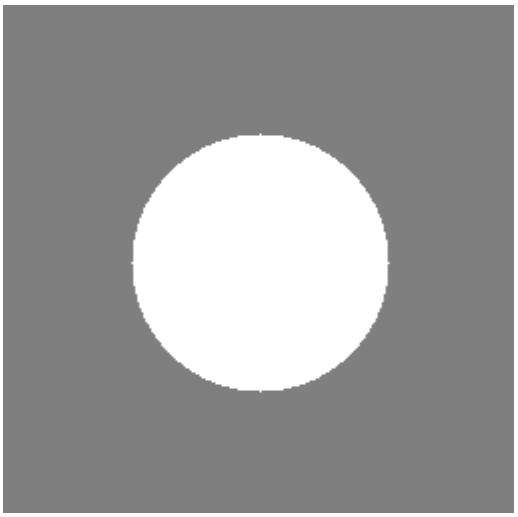

Fig. (a) Circular grain inside another at t=0,

Fig. (b) At t=5000,

ISSN: 0971-1260

Vol-22-Issue-17-September-2019

Fig. (c) At t=10000,

Fig. (d) At t=12000,

### 3.2 Positions and Velocities of boundaries

In Fig. 3.2(i), we show the profile of the request parameter from the centre of the simulation cell to the end of the simulation cell boundary (to the right) at various times.

ISSN: 0971-1260

Vol-22-Issue-17-September-2019

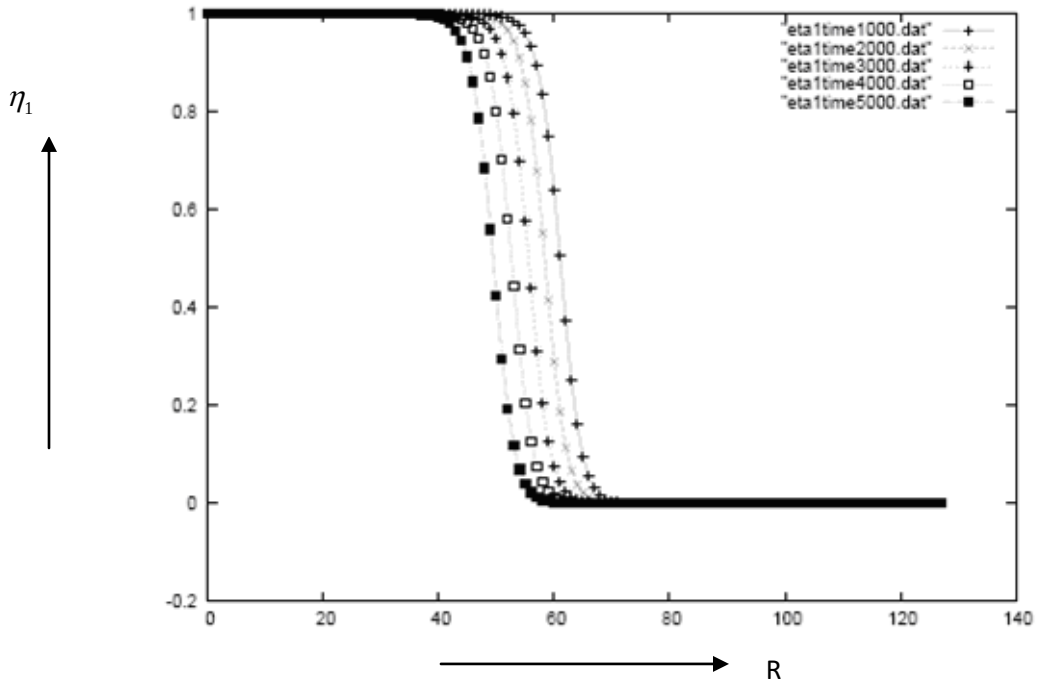


Fig.3.2(i) Graph of order parameter versus position at different times.

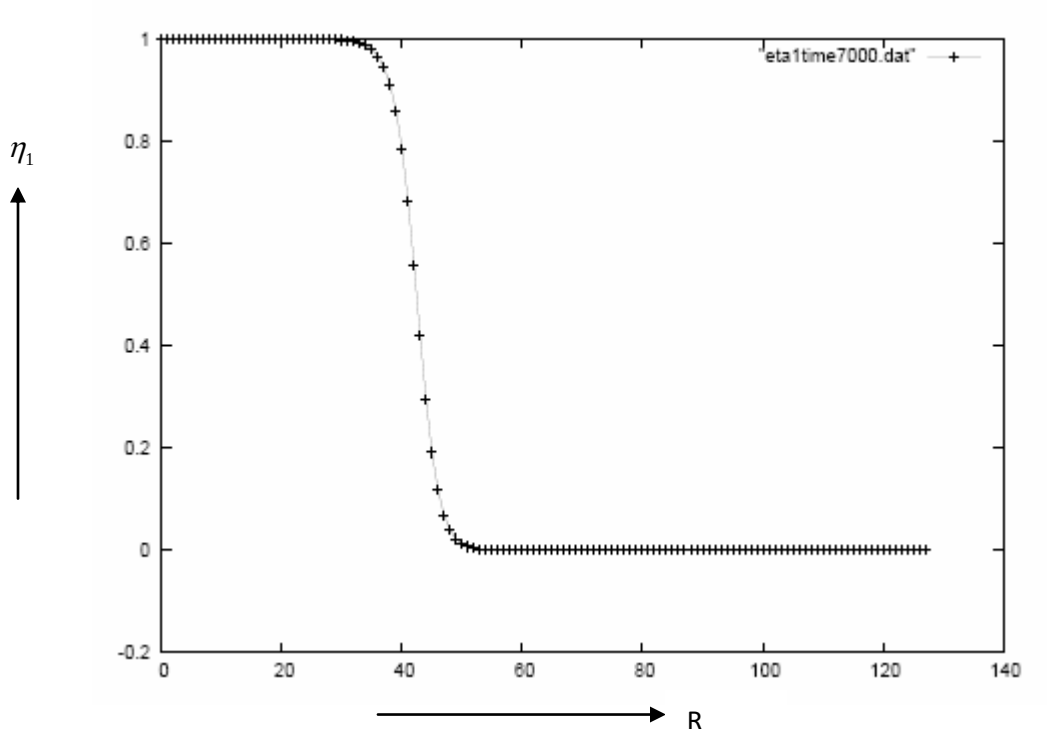

ISSN: 0971-1260

Vol-22-Issue-17-September-2019

Fig.3.2(ii) The profile of the interface at t=7000 for a circular embedded grain.

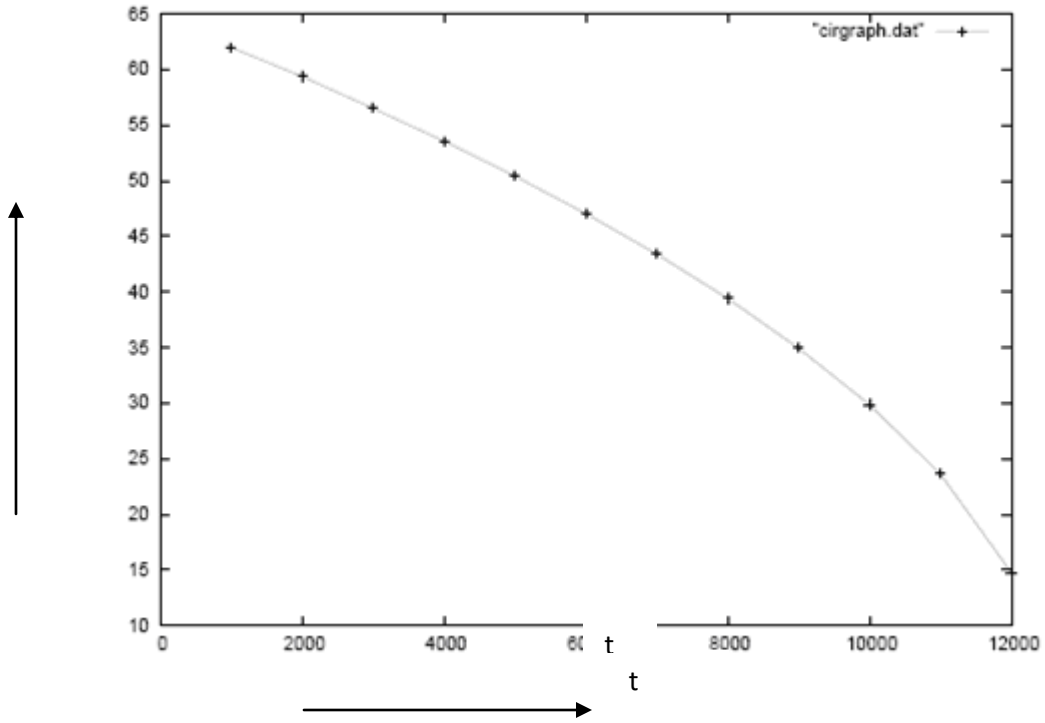


Fig.3.3(iii) Graph of interface position (R) versus time (t) for a circular grain.

From these profiles of the orientation order parameter at different times, we can determine the radius of the shrinking circular grain as a function of time. Let us, for example, consider the profile of the orientational order parameter at time t=7000. This profile is shown in Fig.3.2(ii). From this profile, we identify two points – one above 0.5 and another below 0.5. Knowing the values of the grid position for these two points and the values of the order parameter at these two grid positions, one can calculate the exact point of the grid at which the order parameter profile takes a value of 0.5. For example, in the figure shown above, we have taken the grid point 42 and 44; for these two points, the values of the order parameter, read from the data files are 0.6835766

ISSN: 0971-1260

Vol-22-Issue-17-September-2019

and 0.4215244 respectively. Now, knowing two points, say, $(x_1, y_1)$ and $(x_2, y_2)$, a straight line can be fit using the following expression;

$$x = \frac{x_2 - x_1}{y_2 - y_1}(y - y_1) + x_1 .$$

In other words, we use a straight line interpolation to identify the interface position, which is arbitrarily taken to be the point at which the order parameter takes a value of 0.5. Doing such an analysis on the order parameter profiles and identifying the interface position at each time, we obtain the plot the circular grain radius as a component of time, check in Fig. 3.3(iii).

Once we have the position as a component of time it is rather straight forward to calculate the velocity of the boundary. Further, in the case of the circular boundary we can also calculate the mean curvature corresponding to the velocity by averaging the reciprocal of the radii at the two times which were used to calculate the velocity. That is we calculate the interface velocity (dR/dt) and the mean curvature (1/R), and we show the plot of curvature versus velocity in Fig.3.8. Note that the plot is a straight line barring some deviations at the early stages of the simulation where a diffuse interface is being formed. Thus our numerical results are in agreement with the analytical expression given in the introduction, namely, $V \propto \frac{1}{R}$

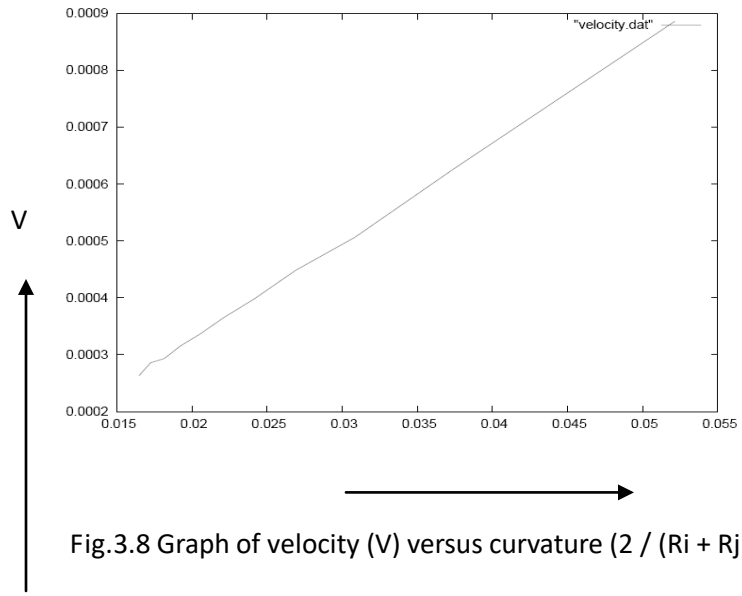


Fig.3.8 Graph of velocity (V) versus curvature (2 / (Ri + Rj)) for circular.

ISSN: 0971-1260

Vol-22-Issue-17-September-2019

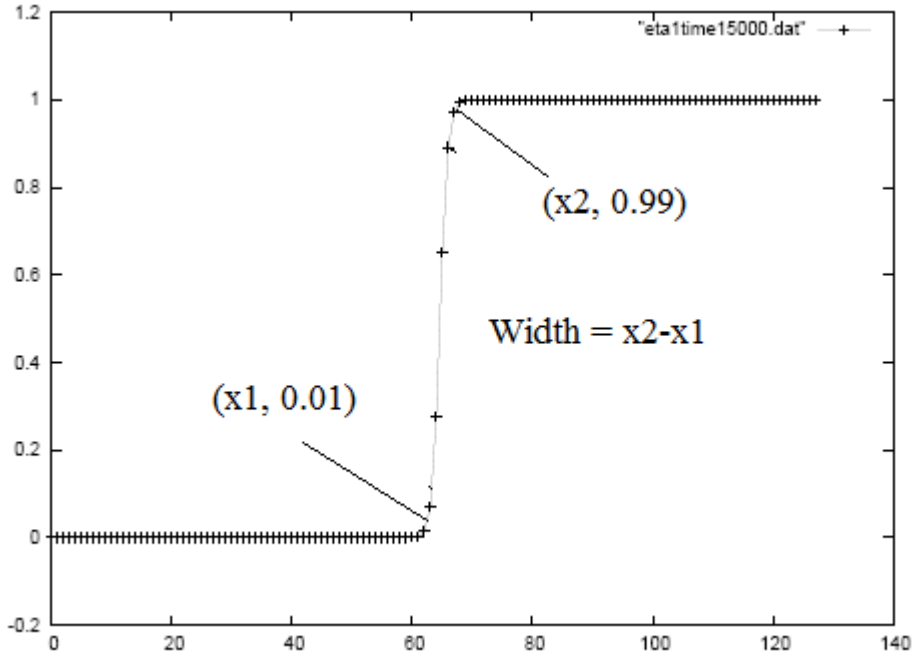


Fig.3.9 Interface profile for determining the width of the interface.

### 3.3 Widths and Energies of the boundaries

In Table 3.1 we show the effect of grid refinement as well as gradient energy coefficient on the interface widths. In this case we consider the flat grain boundary to avoid any errors due to the grain boundary movement. After the boundary becomes diffuse, say after 15000 time steps, we consider the interface profile (see Fig. 3.9). From this profile, we identify two points – one above 0.5 and another below 0.5. Knowing the values of the grid position for these two points and the values of the order parameter at these two grid positions, one can calculate the exact point of the grid at which the order parameter profile takes a value of 0.99 and 0.01. For example, in the figure shown above, we have taken the grid point 65 and 67; for these two points, the value of the order parameter, read from the data files are 0.3655870 and 0.7290936 respectively. Now, knowing two points, say, $(x_1, y_1)$ and $(x_2, y_2)$, a straight line can be fit; or, in other words, we use a straight line interpolation to identify the interface position, put y = 0.99, we get x = 68.43549746. Also put y = 0.01, we get x = 63.04357335. The difference between these two values gives the width of the interface.

ISSN: 0971-1260

Vol-22-Issue-17-September-2019

In Table 3.1, we show the calculated interface widths for three pairs of gradient energy coefficients (see the columns 3-5). It is well known that in this models the interface width scales as the square root of the gradient energy coefficient (see Ref. 14 for example). In Table 3.2 we give the scaled widths ($\frac{w}{k^{0.5}}$) for the different simulations. From these values it is clear that the numerical simulations (a) are not well resolved for $k_1 = k_2 = 1$; (b) the finer discretization of the grids leads to better values. Further from these values it is also clear that for $k_1 = k_2 = 4$ and $k_1 = k_2 = 8$, even a coarse grid gives reliable widths.

**Table 3.1**

**Calculation of the grain boundary width with different value of gradient energy coefficients.**

| Total Grid Size; n_x = n_y<br>Grid Spacing: $\Delta x = \Delta y$<br>Relaxation Coefficients- $L_i$ | Gradient Energy Coefficients $k_i$ | 256<br>$\Delta x = \Delta y = 1$<br>$L_1 = L_2 = 1$ | 512<br>$\Delta x = \Delta y = 0.5$<br>$L_1 = L_2 = 1$ | 1024<br>$\Delta x = \Delta y = 0.25$<br>$L_1 = L_2 = 1$ |
|---|---|---|---|---|
| | $K_1 = K_2 = 1$ | 3.193146075 | 5.3919256 | 11.67026495 |
| | | 5.39192411 | 10.24001336 | 20.99285939 |

ISSN: 0971-1260

Vol-22-Issue-17-September-2019

| | | | | |
|---|---|---|---|---|
| Width | $K_1 = K_2$ =4 | 7.36703627 | 14.96650479 | 29.370556 |
| | $K_1 = K_2$ =8 | | | |

**Table 3.2**

**Scaled grain boundary widths**

| Total Grid Size: n_x = n_y<br>Grid Spacing: $\Delta x = \Delta y$<br>Relaxation Coefficients- $L_i$ | Gradient Energy Coefficients $k_i$ | 256<br>$\Delta x = \Delta y$ =1<br>$L_1 = L_2$ =1 | 512<br>$\Delta x = \Delta y$ =0.5<br>$L_1 = L_2$ =1 | 1024<br>$\Delta x = \Delta y$ =0.25<br>$L_1 = L_2$ =1 |
|---|---|---|---|---|
| | $K_1 = K_2$ =1 | 3.19 | 5.39 | 11.67 |
| | | 2.69 | 5.12 | 10.44 |

ISSN: 0971-1260

Vol-22-Issue-17-September-2019

| | | | | |
|---|---|---|---|---|
| Scaled width | $K_1 = K_2 = 4$ | 2.60 | 5.29 | 10.38 |
| | $K_1 = K_2 = 8$ | | | |

The grain limit vitality starts from the slope vitality terms $(\nabla \eta_i)^2$ which are not zero only in region of the grain boundaries and the local free energy density which has higher values compared to the interior regions of the grain. According to Cahn and Hilliard (see Ref. 15 for example), the energy $\sigma_{gb}$ of flat grain-boundary among orientation *i* & j ($i \neq j$) described as:

$$\sigma_{gb} = \int_{-\infty}^{+\infty} [f_0(\eta_i, \eta_j) - f_{\min} + \frac{k_i}{2}(\frac{d\eta_i}{dx})^2 + \frac{k_j}{2}(\frac{d\eta_j}{dx})^2] dx,$$

Where $f_{\min}$ is the local free energy density in the interior regions of the grain. Note that the grain-boundary energy, thus, is nothing but the extra free energy of in-homogeneous systems than a homogeneous system with an equilibrium value of either $\eta_i$ or $\eta_j$. For a given $f_o$, the boundary energy and thickness vary with $k_i$ and $k_j$. The smaller the $k_i$ and $k_j$, thinner is the boundary region, and smaller is boundaries between different grains.

## 4. Conclusions

1. We have implemented a Fourier spectral code in C to do diffuse interface simulations of 2-D grain growth.

ISSN: 0971-1260

Vol-22-Issue-17-September-2019

**2.** Our numerical simulations are in adequate responses along with some of available analytical results; for example, the growth is curvature driven and the velocity of the boundary is proportional to the curvature.

## 3. References

1. URL:http://www.cartage.org.lb/en/themes/Sciences/Physics/SolidStatePhysics/AtomicBonding/CrystalStructure/Crystalline/Image486.gif.
2. Neumann, J.Von., 1952, "Discussion: Grain shapes and other metallurgical applications of topology", Metal Interfaces, American Society for Metals, Cleveland, Ohio, pp. 108-110.
3. Mullins, W.W., 1956, "Two-dimensional motion of idealized grain boundaries", Journal of Applied Physics, Volume 27, pp. 900-904.
4. Novikov, Yu.V., 1998, "Abnormal grain growth: computer simulation", Interface Science, Volume 6, pp. 77-84.
5. Atkinson, H.V., 1988, "Theories of normal grain growth in pure single phase systems", Acta Metallurgica, Volume 36, pp. 469–491.
6. Glazier, J.A., 1990, "Coarsening in the two-dimensional soap froth and the large-Q Potts model: A detailed comparison", Philosophical Magazine B, Volume 62, pp. 615-645.
7. Fradkov, V.E., Glicksman, M.E., Palmer, M., Nordberg, J., and Rajan, K., 1993, " Topological rearrangements during 2D normal grain growth", Physica D, Volume 66, pp. 50-60.
8. Allen, S.M., and Cahn, J.W., 1979, "A microscopic theory for antiphase boundary

motion and its application to antiphase domain coarsening", Acta Metallurgica, Volume 27, pp. 1085-1095.

9. Fan, D. and Chen, L.Q., 1997, "Diffuse-interface description of grain boundary motion", Philosophical Magazine Letters, Volume 75, No. 4, pp. 187-196.

10. Chen, L.Q., and Yang, W., 1994, "Computer-simulation of the domain dynamics of a quenched system with a large number of nonconserved order parameters - the grain growth kinetics", Physical Review B, Volume 50, pp. 15752-15756.

11. Chen, L.Q., 1995, "A novel computer simulation technique for modelling grain growth", Scripta Metallurgica et Materialia, Volume 32, No. 1, pp. 115-120.

12. Fan, D. and Chen, L.Q., 1997, "Computer simulation of grain growth using a continuum field model", Acta Materialia, Volume 45, No. 2, pp. 611-622.

13. URL:http://gururajan.mp.googlepages.com/phase-field/ch-muse.

14. Haider, F. and Abinandanan, T.A., 2001, "An extended Cahn-Hilliard model for interfaces with cubic anisotropy", Philosophical Magazine, A, Volume 81, No. 10, pp. 2457-2479.

15. Cahn, J.W., and Hilliard, J.E., 1958, "Free energy of a nonuniform system.I. Interfacial energy", Journal of Chemical Physics, Volume 28, No. 2, pp. 258-267.

16. Moelans, N., Blanpain, B., and Wollants, P., 2008, "An introduction to phase-field modeling of microstructure evolution", Computer Coupling of Phase Diagrams and Thermochemistry, Volume 32, pp. 268-294.

 